Indonesian Journal of Science & Technology

Journal homepage: http://ejournal.upi.edu/index.php/ijost/

Structural Characterization, Hirshfield Surface Analysis, and Molecular Docking of Novel Diquinoline Derivatives as Anti-Tumor Agents

Solhe F. Alshahateet[1,], Salah A. Al-Trawneh[1], Safaa Hidaoui[2], Er-rajy Mohammed[2], Mohammed Zerrouk[2], Yousef M. Al-Saraireh[1], Waad M. Al-Tawarh[1], Mohammad S. Hareedy[1,3], Ahmed A. Al-abadleh[4], Tala S. Alshahateet[4], Khalil Azzaoui[2,5], Belkheir Hammouti[6], Ismail Warad[7]*

[1]Mutah University, Al-Karak 61710, Jordan
[2]University Sidi Mohamed Ben Abdellah, Fez 30000, Morocco
[3]Assiut University, Assiut, Egypt
[4]Al-Karak Governmental Hospital, Ministry of Health, Al-Karak 11118, Jordan
[5]SUPMTI, Rabat, Morocco
[6]Euromed University of Fes, UEMF, Fes 30030, Morocco
[7]An-Najah National University, Nablus, Palestine
*Correspondence: E-mail: s_alshahateet@mutah.edu.jo

ABSTRACT

Quinoline is a versatile scaffold in anticancer drug design due to its structural flexibility and diverse biological activity. This study reports the synthesis, characterization, Hirshfeld surface analysis, molecular docking, and cytotoxic evaluation of three novel diphenyldiquinoline derivatives: DPDQ-3a, DNDPDQ-3b, and DCDPDQ-3c. The compounds were synthesized via Friedländer condensation and tested against lung (A549), colorectal (DLD1), and breast (MCF-7) cancer cells, with human embryonic kidney (HEK293) as controls. DPDQ-3a showed the strongest potency and selectivity, with IC_{50} values lower than cisplatin and reduced toxicity toward normal cells. Hirshfeld analysis revealed stabilizing intermolecular interactions, while docking studies confirmed high binding affinities to cancer-related proteins. In silico toxicity assessment indicated favorable safety, highlighting DPDQ-3a as a promising anticancer candidate.

ARTICLE INFO

Article History:
Submitted/Received 24 May 2025
First Revised 20 Jun 2025
Accepted 24 Aug 2025
First Available Online 27 Aug 2025
Publication Date 01 Apr 2026

Keyword:
Anti-tumor agents,
Cytotoxicity,
Diphenyldiquinoline (DPDQ),
Disease prevention,
Good health and well-being,
Health promotion,
In silico toxicity,
Medical innovation,
Molecular docking,
Public health,
Quinoline derivatives.

1. INTRODUCTION

Cancer remains one of the leading causes of death and a major global health challenge, claiming millions of lives each year despite significant advances in diagnosis and treatment. Many reports regarding cancer and how to fight them are well-documented [1-5]. Chemotherapy continues to be widely used, yet it is often associated with severe side effects and limited selectivity toward tumor cells. This situation underscores the urgent need for new compounds that are both more effective and less toxic. In this context, heterocyclic compounds (particularly quinoline derivatives) have shown remarkable promise in drug development due to their versatile biological activities and structural tunability, making them excellent candidates for therapeutic design [6].

The anticancer potential of quinoline derivatives has been demonstrated through several mechanisms, including induction of apoptosis, inhibition of angiogenesis, and disruption of key enzymatic and signaling pathways necessary for tumor growth and metastasis. Their flexible molecular framework allows extensive modifications, enabling the development of derivatives with enhanced biological activity. Substituents such as nitro and chloro groups play a crucial role in modulating cytotoxicity, tumor specificity, and pharmacokinetic behavior [7,8].

In recent years, diphenyldiquinoline derivatives have attracted growing interest as potential anticancer agents. Derived through the Friedländer condensation, these compounds combine quinoline and phenyl moieties, conferring favorable pharmacological properties [9,10]. Previous studies suggest that structural modifications in these derivatives can significantly improve therapeutic efficacy while reducing off-target effects. Nevertheless, further insights into their structure-activity relationships (SAR) and interactions with biological targets are essential for realizing their full potential [11].

The present study focuses on the synthesis and evaluation of three novel diphenyldiquinoline derivatives (DPDQ-3a, DNDPDQ-3b, and DCDPDQ-3c). Their antiproliferative activity was tested against non-small cell lung cancer (A549), colorectal cancer (DLD1), and breast cancer (MCF-7) cell lines, with cytotoxicity assessed in normal human embryonic kidney cells (HEK293). MTT assays were performed to determine IC_{50} values and selectivity indices, using cisplatin as a reference drug.

To support the biological findings, based on previous studies (see **Table 1**), molecular docking studies were conducted to explore the binding potential of the most promising derivatives with tumor-related protein targets. Additionally, in silico toxicity predictions were carried out to evaluate safety profiles, particularly regarding hepatotoxicity, nephrotoxicity, and other potential adverse effects. By integrating experimental and computational approaches, this study provides a comprehensive evaluation of diphenyldiquinoline derivatives as prospective anticancer agents. The significance of this research lies in advancing the development of selective and effective compounds that may contribute to improved cancer therapy.

Table 1. Previous studies on molecular docking.

No	Title	Ref.
1	*Artemisia herba alba* essential oil: GC/MS analysis, antioxidant activities with molecular docking on S protein of SARS-CoV-2	[12]
2	Triazolopyrimidine derivatives: A comprehensive review of their synthesis, reactivity, biological properties, and molecular docking studies	[13]

DOI: https://doi.org/10.17509/ijost.v11i2.89682
p- ISSN 2528-1410 e- ISSN 2527-8045

Table 1 (continue). Previous studies on molecular docking.

No	Title	Ref.
3	Deciphering the mechanism of action *Cosmos caudatus* compounds against breast neoplasm: A combination of pharmacological networking and molecular docking approach with bibliometric analysis	[14]
4	Synthesis, antibacterial evaluation and molecular docking of 2,4,5-tri-imidazole derivatives	[15]
5	Reverse docking on five original PPO structures: Plant, bacterial, and human	[16]
6	Synthesis, optimization, DFT/TD-DFT and COX/LOX docking of new Schiff base N'-((9-ethyl-9H-carbazol-1-yl)methylene)naphthalene-2-sulfonohydrazide	[17]
7	Synthesis, characterization, E/Z-isomerization, DFT, optical and IBNA docking of new Schiff base derived from naphthalene-2-sulfonohydrazide	[18]
8	Design, synthesis, and biological evaluation of new sulfonamides derived from 2-aminopyridine: Molecular docking, POM analysis, and identification of the pharmacophore sites	[19]
9	Computational approaches to *Spirulina platensis* growth with urea-derived nanonutrients: Thermodynamic properties, energetic profiles, molecular docking and POM analysis	[20]
10	Preparation and characterization of new mixed azo ligand complexes with some metal ions and in vitro biological activity and molecular docking study of Ni(II) and Hg(II) complexes	[21]
11	Molecular docking studies for the identifications of novel antimicrobial compounds targeting *Staphylococcus aureus*	[22]
12	Potential inhibition of ALDH by argan oil compounds, computational approach by docking, ADMET and molecular dynamics	[23]
13	3D-QSAR, molecular docking, molecular dynamic simulation, and ADMET study of bioactive compounds against *Candida albicans*	[24]
14	Acetylcholinesterase, tyrosinase, α-glucosidase inhibition of *Ammoides leucotrichus* fruits essential oil and ethanolic extract and molecular docking analysis	[25]
15	3D-QSAR modeling, molecular docking and drug-like properties investigations of novel heterocyclic compounds derived from *Magnolia officinalis* as hit compounds against NSCLC	[26]
16	Novel triazole-pyrazine as potential antibacterial agents: Synthesis, characterization, antibacterial activity, drug-likeness properties and molecular docking studies	[27]
17	Investigating the biological activities of Moroccan *Cannabis sativa* L. seed extract: Antimicrobial, anti-inflammatory, and antioxidant effects with molecular docking analysis	[28]
18	Investigation of the usability of some triazole derivative compounds as drug active ingredients by ADME and molecular docking properties	[29]
19	In silico design of new α-glucosidase inhibitors through 3D-QSAR study, molecular docking modeling and ADMET analysis	[30]
20	In search of new potent α-glucosidase inhibitors: Molecular docking and ADMET prediction	[31]
21	In silico studies of 1,4-disubstituted 1,2,3-triazole with amide functionality: Antimicrobial evaluation against *Escherichia coli* using 3D-QSAR, molecular docking, and ADMET properties	[32]
22	Deciphering the SARS-CoV-2 Delta variant: Antiviral compound efficacy by molecular docking, ADMET, and dynamics studies	[33]
23	In silico docking, drug-likeness and toxicity prediction studies of bioactive compounds of *Eurycoma longifolia* as potential multi-targeted antiviral agents against SARS-CoV-2	[34]
24	Extract and molecular docking: Exploring the oxidation of 3,5-di-tert-butylcatechol and 2-aminophenol in the presence of O_2 from air	[35]
25	Synthesis, structural and crystallographic characterization of new hydrosoluble thymol derivatives with enhanced antioxidant activity assessed by docking study	[36]
26	Synthesis, anticancer, antimicrobial evaluation, in silico molecular docking and POM analyses of new 4,7-dimethyl coumarin containing sulfonamides	[37]

DOI: https://doi.org/10.17509/ijost.v11i2.89682
p- ISSN 2528-1410 e- ISSN 2527-8045

Table 1 (continue). Previous studies on molecular docking.

No	Title	Ref.
27	Synthesis, spectroscopic characterization, cytotoxic activity, ADME prediction and molecular docking studies of the novel series quinoxaline-2,3-dione	[38]
28	Molecular docking and ADMET prediction of compounds from *Piper longum* L. detected by GC-MS analysis in diabetes management	[39]
29	CoMFA topomer, CoMFA, CoMSIA, HQSAR, docking molecular, dynamique study and ADMET study on phenoxypropyl isoxazole derivatives for coxsackie virus B3 inhibitors activity	[40]
30	Computational insights into benzothiophene derivatives as potential antibiotics against multidrug-resistant *Staphylococcus aureus*: QSAR modeling and molecular docking studies	[41]

2. METHODS

2.1. Synthesis of Diquinoline Derivatives

The synthetic pathway of the diquinoline derivatives is illustrated in **Figure 1**. All compounds were prepared using the Friedländer condensation reaction, as previously described [42,43]. The synthesis of several materials is in the following:

(i) Diphenyldiquinoline (DPDQ-3a). 2-Aminobenzophenone (2 equivalents) and bicyclo[3.3.1]nonane-3,7-dione (1 equivalent) were dissolved in 20 mL of absolute ethanol, followed by the addition of 2 mL of 10 M HCl. The mixture was refluxed overnight, then filtered and washed with ice-cold ethanol. The light brown powder obtained corresponded to DPDQ, with a yield of 73%.

(ii) Dinitrodiphenyldiquinoline (DNDPDQ-3b). 2-Amino-5-nitrobenzophenone (2 equivalents) and bicyclo[3.3.1]nonane-3,7-dione (1 equivalent) were dissolved in 20 mL of ethanol with 2 mL of HCl. The solution was refluxed overnight, filtered, and washed with ice-cold ethanol. The product was collected as an off-white solid, with a yield of 50%.

(iii) Dichlorodiphenyldiquinoline (DCDPDQ-3c). 2-Amino-5-chlorobenzophenone (2 equivalents) and bicyclo[3.3.1]nonane-3,7-dione (1 equivalent) were dissolved in 20 mL of ethanol, followed by 2 mL of HCl. The mixture was refluxed overnight, filtered, and washed with ice-cold ethanol. The reaction produced a light orange powder, with a yield of 92%.

2.2. Hirshfeld Surface Analysis

Hirshfeld surface (HS) analysis was employed to investigate intermolecular interactions in the crystal structures of DPDQ-3a, DNDPDQ-3b, and DCDPDQ-3c. The analysis was performed using Crystal Explorer software [44]. The normalized contact distance (dnorm) was calculated from the internal (di) and external (de) atomic distances relative to their van der Waals radii [45]. It is defined as the distance from the surface to the nearest internal and external atoms and expressed in Equation (1).

$$d_{norm} = \frac{d_i - r_i^{vdW}}{r_i^{vdW}} + \frac{d_e - r_e^{vdW}}{r_e^{vdW}} \quad (1)$$

where r_i^{vdW} and r_e^{vdW} represent the van der Waals radii of atoms inside and outside the surface, respectively. The dnorm values were then mapped onto the Hirshfeld surface using a blue-white-red color scheme, in which blue indicates long contacts, white corresponds to contacts close to the van der Waals separation, and red highlights short contacts [46]. Intermolecular interactions within the crystal lattice were further represented through the combination of di and de in the form of two-dimensional fingerprint plots. These plots were

DOI: https://doi.org/10.17509/ijost.v11i2.89682
p- ISSN 2528-1410 e- ISSN 2527-8045

generated within the range of 0.6-2.4 Å to visualize reciprocal contacts and quantify the contribution of different interaction types.

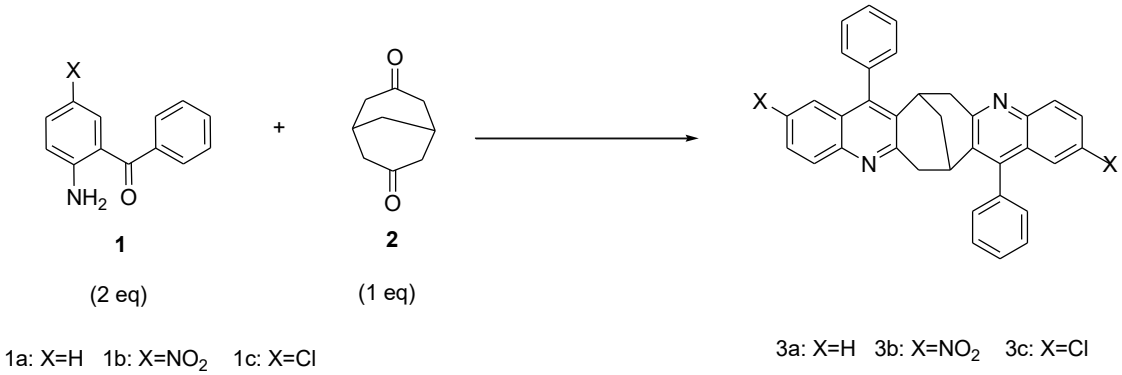

Figure 1. Synthesis of the diphenyldiquinoline derivatives (DPDQ-3a, DNDPDQ-3b, and DCDPDQ-3c).

2.3. Anti-Tumor Activity Experiments

Anti-tumor activity experiments, including:

(i) Cell culture

Human cancer cell lines A549 (lung), DLD1 (colorectal), and MCF-7 (breast), along with normal human embryonic kidney cells (HEK293), were purchased from ATCC. The growth media and supplements were obtained from EuroClone (Milan, Italy). A549, DLD1, and MCF-7 cells were cultured in RPMI 1640 medium supplemented with 2 mM L-glutamine, 1% penicillin-streptomycin, 1% amphotericin B, and 10% fetal calf serum (FCS). HEK293 cells were cultured in DMEM with the same supplements. All cell lines were maintained at 37 °C in a humidified incubator with 5% CO_2. Cells were detached with 0.05% trypsin-EDTA during sub-culturing, and medium was refreshed every 48–72 hours.

(ii) Anti-proliferative activity

The Thiazolyl Blue Tetrazolium Bromide (MTT) assay was used to assess cell viability. Cells were seeded in 96-well plates at a density of 1×10^4 cells/mL and allowed to adhere. Different concentrations of DPDQ derivatives (1, 50, 100, and 200 µM/mL) were added, with cisplatin (1, 25, 50, and 100 µM/mL) used as a positive control. After 96 hours, the medium was replaced with MTT solution (5 mg/mL) and incubated for 4 hours. Formazan crystals were dissolved in DMSO, and absorbance was measured at 620 nm using a multimode reader (Agilent Technologies, USA). All experiments were repeated three times. IC_{50} values were calculated, and the Selectivity Index (SI) was determined as the ratio of IC_{50} in normal cells to IC_{50} in cancer cells. An SI > 3 was considered indicative of selective anticancer activity.

(iii) Morphology analysis

Cell morphology was examined after treatment with each compound at its respective IC_{50} value. Cells were fixed with ice-cold methanol at 4 °C for 30 minutes and stained with hematoxylin. After rinsing and drying, morphological changes were observed using an inverted light microscope at 40× magnification.

(iv) Statistical analysis

Data were expressed as mean ± standard deviation from three independent experiments. Statistical differences between groups were analyzed using a t-test, with $p < 0.05$ considered significant. We analyzed statistics to get a better understanding of

DOI: https://doi.org/10.17509/ijost.v11i2.89682
p- ISSN 2528-1410 e- ISSN 2527-8045

the results. Detailed information on how to analyze using statistical analysis is reported elsewhere [47-49].

2.4. In Silico Toxicity Prediction

Based on cytotoxicity results, DPDQ-3a and DCDPDQ-3c were selected for toxicity evaluation using the ProTox-II webserver [50,51]. Predictions included acute oral toxicity (LD_{50} values), organ-specific toxicity, and various toxicological endpoints.

2.5. Molecular Docking

The synthesized compounds were visualized using ChemDraw 16.0 and optimized with the MM2 method. Docking studies were conducted with the Molecular Operating Environment (MOE) software [52]. Target proteins were retrieved from the Protein Data Bank [53]. Before docking, water molecules were removed, hydrogen atoms added, and missing side chains corrected. Potential energy was minimized using the MMFF94x force field [54-56]. The optimized compounds were saved in MDB format for docking. In this study, DPDQ-3a and DNDPDQ-3b were docked against tumor-related protein targets to assess binding affinity and potential anticancer activity [57,58].

3. RESULTS AND DISCUSSION

3.1. Structural Description or Single X-Ray Diffraction Analysis

3.1.1. Diphenyldiquinoline

This molecule features a multi-cyclic framework with interconnected aromatic and non-aromatic rings. The central structure is a bicyclic system comprising a six-membered aromatic ring fused to a five-membered ring, with the aromatic ring exhibiting alternating double bonds that suggest conjugation and resonance stability (**Figure 2**). Extending from this bicyclic core is a branched aliphatic chain terminating in functional groups, including hydroxyl (-OH) and thiol (-SH) groups, which may contribute to its chemical reactivity or interaction with other molecules. Several additional substituents, such as methyl groups and hydrogen atoms, are attached to the cyclic and aliphatic portions, and their specific spatial arrangements suggest the presence of stereocenters, indicating chirality in the molecule. The sulfur atoms within the thiol groups are likely connected to additional atoms or functional groups, suggesting potential thioether or disulfide linkages. Overall, the molecule's structure combines aromatic, aliphatic, and functional group characteristics, making it a chemically diverse and potentially bioactive compound.

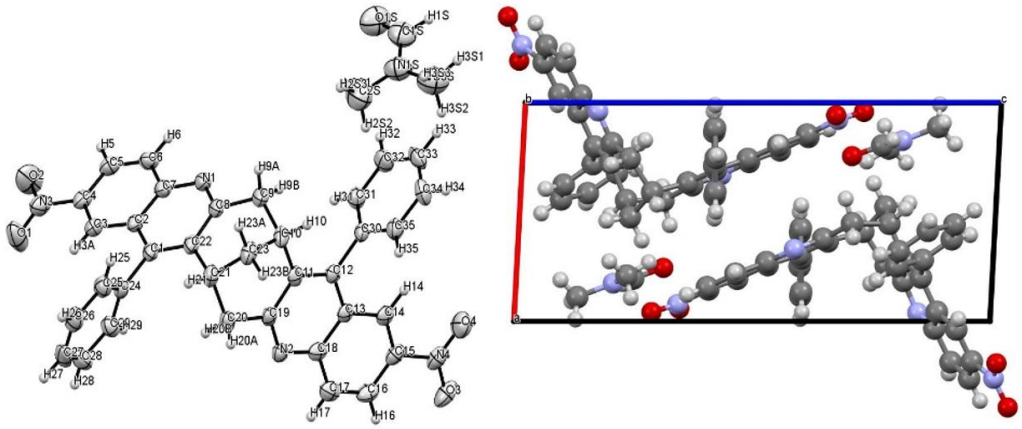

Figure 2. The crystal packing viewed along the direction (101) of Dinitrodiphenyldiquinoline.

DOI: https://doi.org/10.17509/ijost.v11i2.89682
p- ISSN 2528-1410 e- ISSN 2527-8045

3.1.2. Dinitrodiphenyldiquinoline

This molecule displays a complex structure with a combination of cyclic and acyclic components, showcasing both aromatic and aliphatic regions (**Figure 3**). The core of the molecule includes a central bicyclic system, where one six-membered ring is fused with another six-membered or five-membered ring. The aromaticity of one or more rings is evident through alternating double bonds, indicative of conjugation.

Attached to this bicyclic core is a branched aliphatic chain that incorporates several functional groups. Hydroxyl (-OH) groups and other polar groups, such as sulfur-containing thiol (-SH) or sulfoxide groups, appear to be present, suggesting potential reactivity or functional diversity. The structure also features additional rings or substituents extending from the main framework, with various hydrogen atoms, methyl groups, and stereocenters labeled, indicating chirality.

The arrangement of bonds, including single, double, and possible aromatic bonds, highlights the molecule's intricate three-dimensional conformation. This molecule's structure, with its combination of functional groups and cyclic systems, suggests it could have applications in organic synthesis, catalysis, or bioactivity studies.

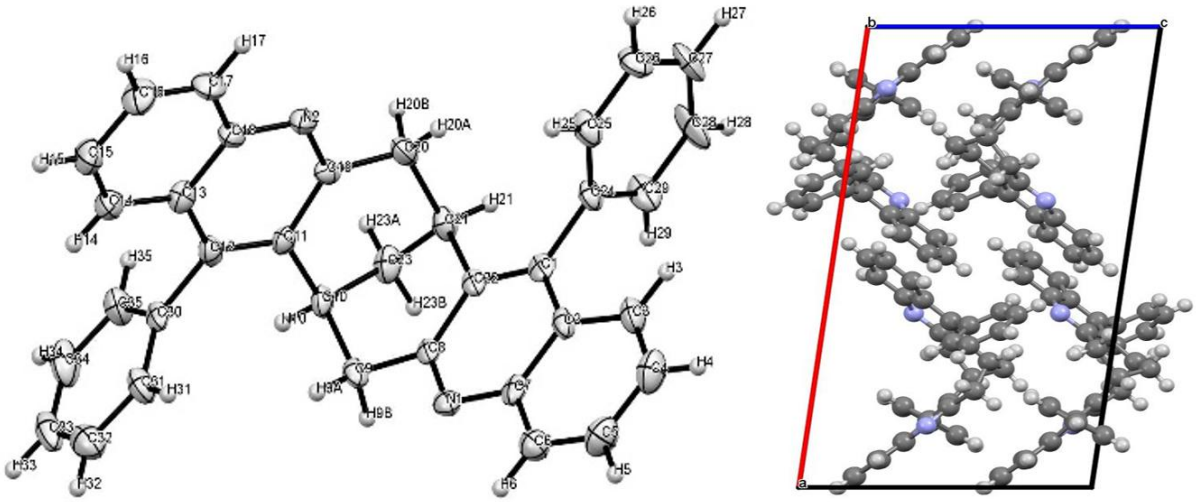

Figure 3. The crystal packing viewed along the direction (101) of Diphenyldiquinoline.

3.1.3. Dichlorodiphenyldiquinoline

The molecule depicted is a structurally complex organic compound featuring both aromatic and aliphatic regions (**Figure 4**). It contains two chlorine atoms, highlighted in green, attached to different parts of the molecule, likely enhancing its chemical reactivity or stability. A nitrogen atom (N1) is incorporated into the structure, indicating the presence of a nitrogen-containing functional group, such as an amine or imine. The molecule's architecture includes a combination of planar aromatic rings and branched aliphatic chains, providing structural diversity. Additionally, the spatial arrangement of bonds and substituents suggests the presence of chiral centers, highlighting the potential for stereoisomerism. This level of functionalization and stereochemical complexity implies that the molecule could have applications in medicinal chemistry, catalysis, or material science, depending on its specific properties.

DOI: https://doi.org/10.17509/ijost.v11i2.89682
p- ISSN 2528-1410 e- ISSN 2527-8045

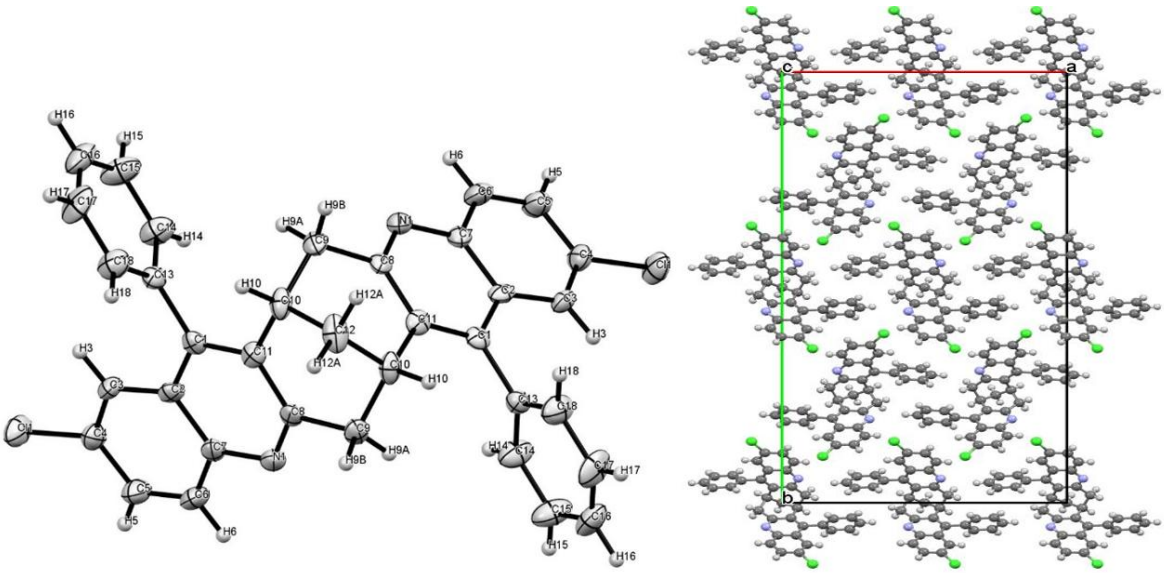

Figure 4. The crystal packing viewed along the direction (110) Dichlorodiphenyldiquinoline.

3.2. Intermolecular Interactions Calculations

Hirshfeld surface analysis and 2D fingerprint plots were used to visualize intermolecular interactions that ensure the cohesion of the crystal structures, identifying each type of intermolecular interaction. The 3D dnorm surfaces were generated at high resolution over a fixed color scale of −0.1293 (red) to 1.3355 Å (blue) for DPDQ-3a (**Figure 5(a)**), −0.1804 (red) to 1.6558 Å (blue) for DNDPDQ-3b (**Figure 5(d)**), and −1.2664 (red) to 1.1712 (blue) Å for DCDPDQ-3c (**Figure 5(g)**). The red spots in the dnorm map correspond to the closest intermolecular interactions [59-61]. Furthermore, in the shape index map, red and blue regions represent the donor and acceptor groups, respectively. It is important to highlight that the the appearance of neighboring blue and red triangles in the shape index surface confirms the interactions resulting from π-stacking, which can be seen as black circles in **Figure 5(e)**. Turning to the curvature map, the bright red cavities revealed concave regions caused by the carbon atoms of the π-stacked molecule situated outside the surface, while the green and blue regions provide visual insights into the planarity and curvature of the molecule.

The distribution of the different intermolecular interactions, based on the HS analysis of the studied compounds, is displayed in **Figure 6**. Fingerprint plots of 3a, 3b, and 3c are shown in **Figures 7, 8, and 9**, respectively, and illustrate the intermolecular contacts present in the crystalline solid. The analysis showed that H···H interactions had the the highest contribution, representing 57, 44.5, and 46.7% of the total surface area in compounds 3a, 3b and 3c, respectively. The prevalence of H···H contacts can be assigned to the small van der Waals radii of hydrogen atoms, signifying the shortest distance on the surface [62].

Furthermore, the other prominent intermolecular contacts were C···H/H···C interactions, which primarily came from C-H···π (ring) in compounds 3a and 3c, accounting for 33% and 22.2%, respectively. In contrast, O··· H/H···O contacts made up 25.1% in compound 3b. Other interactions contributed as follows : N...H (8%), C...C (1.3%), C...N/N...C (0.7%) in compound 3a; C...H/H...C (12.8%), N...H/H...N (5.5%), C...C (5.4%), C...N/N...C (1.2%) in compound 3b; and Cl...H/H...Cl (13.8%), C...C (9%), N...H/H...N (3.6%), N...Cl/Cl...N (2.8%), Cl...C/C...Cl (2.1%) in compound 3c.

DOI: https://doi.org/10.17509/ijost.v11i2.89682
p- ISSN 2528-1410 e- ISSN 2527-8045

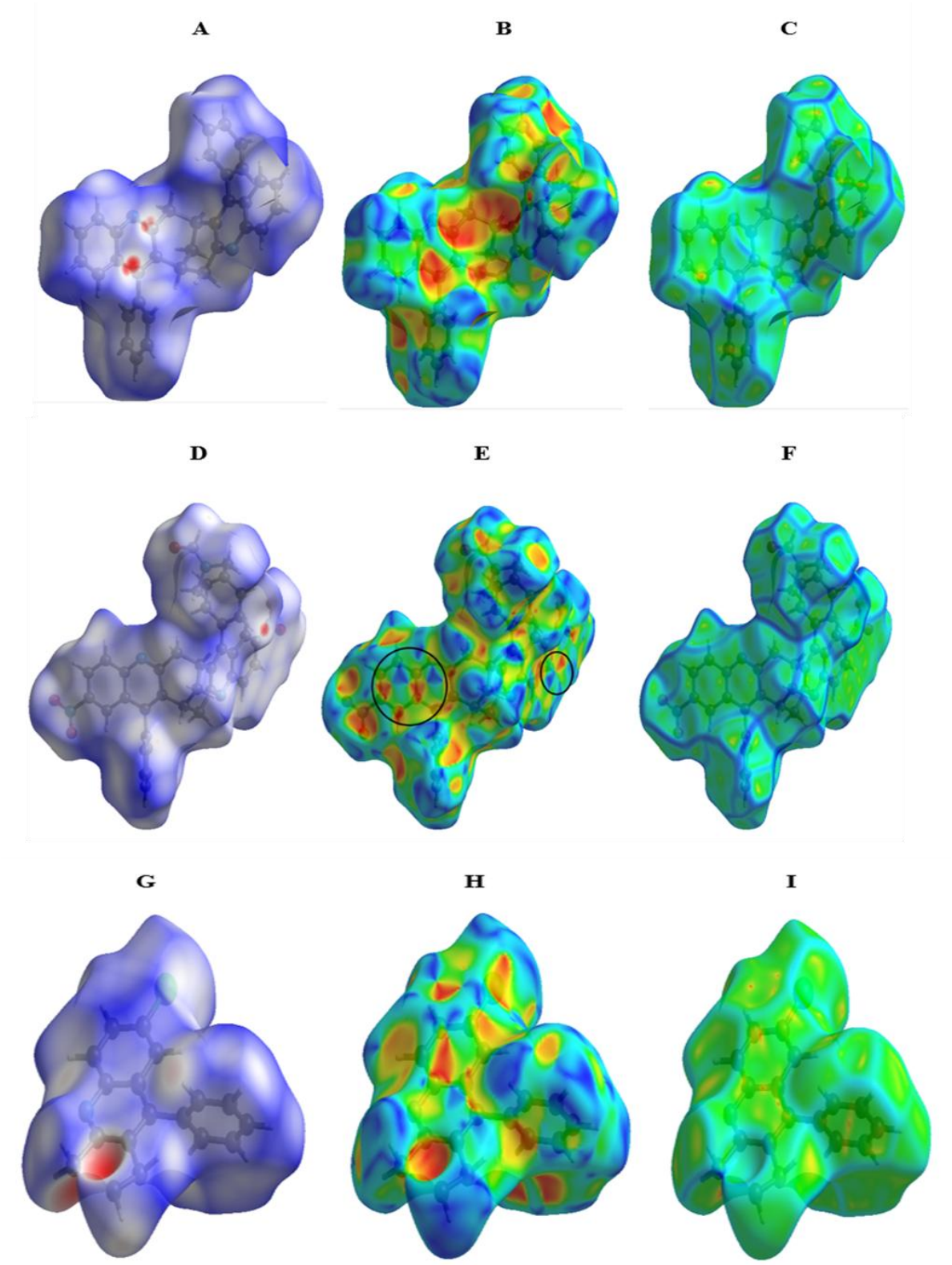

Figure 5. Hirshfeld surface mapped with dnorm (a), shape index (b), and curvedness (c) for compound (DPDQ)-3a; dnorm (d), shape index (e), and curvedness (f) for compound (DNDPDQ)-3b; and dnorm (g), shape index (h), and curvedness (i) for compound (DCDPDQ)-3c.

DOI: https://doi.org/10.17509/ijost.v11i2.89682
p- ISSN 2528-1410 e- ISSN 2527-8045

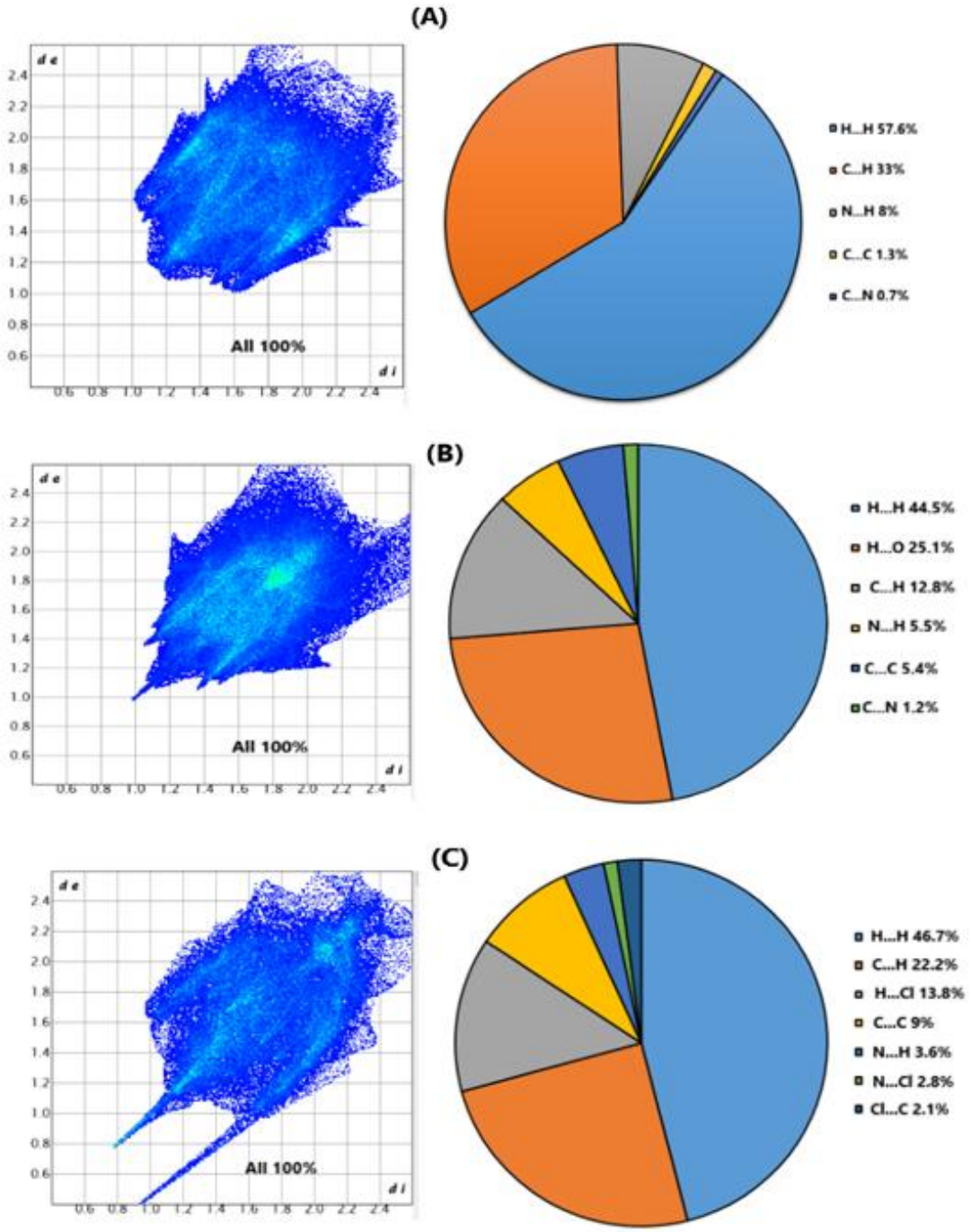

Figure 6. Percentage contributions of interatomic interactions to the HS for (a) compound (DPDQ)-3a, (b) compound (DNDPDQ)-3b, and (c) compound (DCDPDQ)-3c.

DOI: https://doi.org/10.17509/ijost.v11i2.89682
p- ISSN 2528-1410 e- ISSN 2527-8045

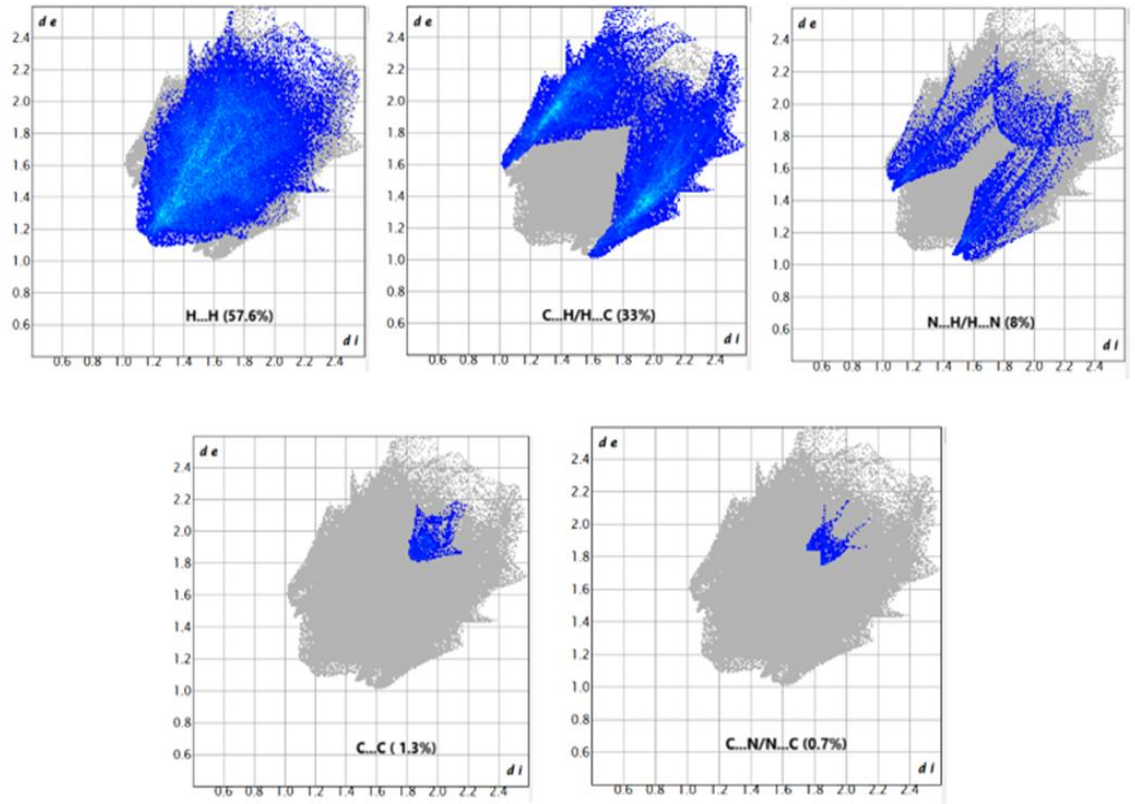

Figure 7. The full 2D fingerprint plots for compound (DPDQ)-3a, showing all interactions. The (de) and (di) values represent the closest external and internal distances from given points on the Hirshfeld surface contacts.

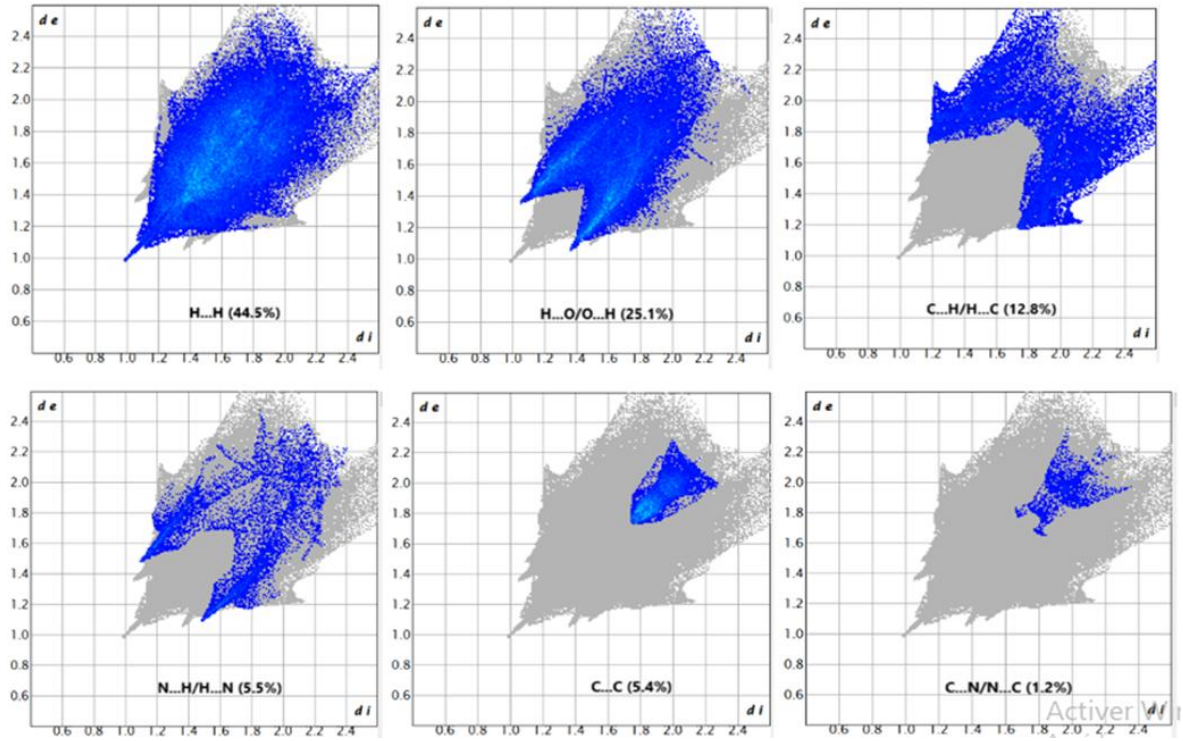

Figure 8. The full 2D fingerprint plots for compound (DNDPDQ)-3b, showing all interactions.

DOI: https://doi.org/10.17509/ijost.v11i2.89682
p- ISSN 2528-1410 e- ISSN 2527-8045

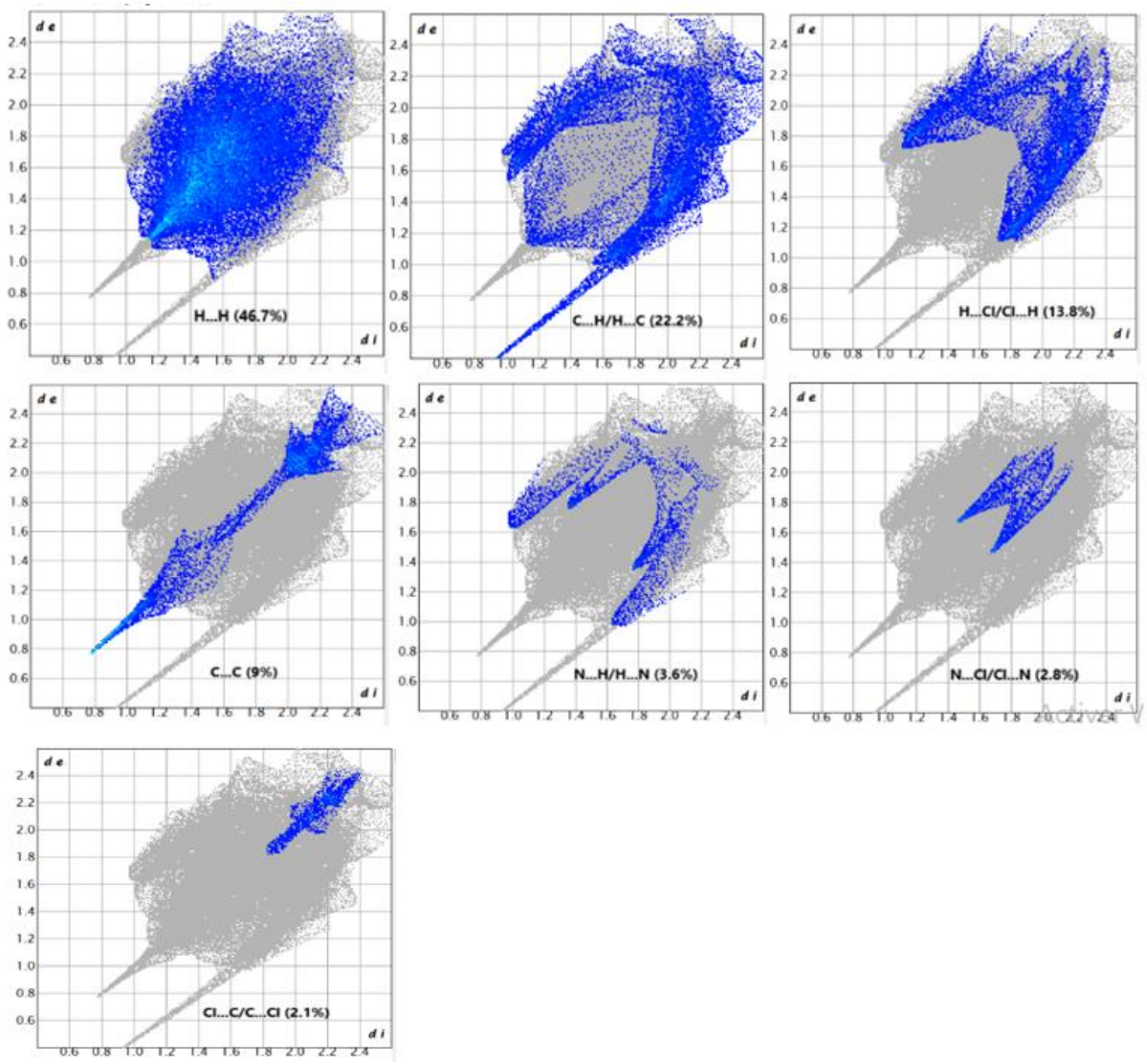

Figure 9. The full 2D fingerprint plots for compound (DCDPDQ)-3c, showing all interactions.

3.3. Anti-Proliferative Activity

Quinoline is a privileged scaffold that has been widely used for the development of new drugs with numerous therapeutic uses. The diversity of quinoline synthetic properties has enabled the development of a broad range of structurally diverse derivatives, thereby enhancing various biochemical and biological applications, particularly cancer therapy [63]. Quinoline derivatives exert their potent anticancer activity through different mechanisms, including but not limited to induction of cell cycle arrest and apoptosis, inhibition of angiogenesis, and enzyme pathways like tyrosine kinases, and disruption of cell invasion and migration. Therefore, the ability of quinoline derivatives to preferentially attack tumor enzyme pathways and tumor-specific signals remains essential for developing safe and effective anticancer treatments [64]. On this basis, the rationale for synthesizing DPDQ derivatives (3a-c) with either dichloro or dinitro substitutions may potentially offer high synergistic anti-cancer activity with minimal clinical toxicity for cancer patients.

Results showed that all DPDQ derivatives (3a-c) exhibited dose-dependent cytotoxicity towards all cell lines, though to varying degrees (**Figure 10** and **Table 2**). Compared to normal cells (HEK293), DPDQ (3a) and DCDPDQ (3c) displayed a significantly potent cytotoxic effect

DOI: https://doi.org/10.17509/ijost.v11i2.89682
p- ISSN 2528-1410 e- ISSN 2527-8045

against various cancer cell lines. However, DPDQ (3a) derivative exhibited higher potency and best selectivity than DCDPDQ (3c) towards all types of cancer cells relative to normal cells. Significantly, the DPDQ (3a) IC50 concentration for every cancer cell line was lower than that of the reference drug cisplatin for the respective cancer cell line [IC50 = 8.7±1.8 µM/ml (DLD1); 7.9±2.2 µM/ml (MCF-7) and 9±3.6 µM/ml (A549) ($p \leq 0.001$)], suggesting that DPDQ has greater anti-cancer activity than the reference drug. In contrast, DPDQ (3a) was less toxic to normal cells as its IC50 concentration for normal cells was quite greater than cisplatin [IC50 = 38.6±5.1 µM/ml (HEK293), ($p \leq 0.001$)] [58]. Decoration of quinoline scaffold with a phenyl moiety at the pyridine ring was shown to be an important factor for synergistic anticancer activity [64]. Importantly, the addition of chloro atoms at both benzene rings, as in the case of DCDPDQ (3c), preserved the cytotoxic activity and selectivity for only the lung cancer cell line (A549), while cytotoxic activity was reduced by almost double in other cancer cell lines. This is consistent with a previous study showing that halogenation of the phenylquinoline moiety, particularly chlorine, has led to reduced anticancer activity in particular cancer cell lines like MCF-7 [64]. Interestingly, a weak non-selective cytotoxic effect was displayed in cancer cell lines upon replacement of dichloro atoms with dinitro groups, as in the case of DNDPDQ (3b). Upon morphological analysis, treatment of cancer cells with DPDQ derivatives (3a-c) and cisplatin at respective IC50 concentrations led to cell detachment and loss the cellular integrity (**Figure 11**). Cells became rounded and shrunken with a condensed nucleus. Such changes indicate a disruption in the cell cytoskeleton. In contrast, untreated control cells preserved the cellular integrity as a typical spindled shape morphology with a uniform cytoplasm and nucleus.

Table 2. Selectivity index and IC50 values (µM) of DPDQ derivatives and cisplatin in all cell lines treated for 96 hours.

	IC_{50} (µM)				SI		
Drug/ Cell line	**HEK293**	**DLD1**	**MCF-7**	**A549**	**DLD1**	**MCF-7**	**A549**
DPDQ -3a	38.6±5.1	8.7±1.8	7.9±2.2	9±3.6	4.4	4.9	4.3
DCDPDQ- 3c	23.7±4.6	19.3±5.9	14.1±3.8	6.7±2.3	1.2	1.7	3.5
DNDPDQ- 3b	679.8±30.5	339.9±21.8	445.7±27.4	276.9±25.1	2	1.5	2.5
Cisplatin	19.61±4.8	11.8±3.9	12±3.1	10±2.2	1.7	1.6	2

3.4. In Silico Prediction of Toxicity

The ProTox-II toxicity predictions showed that both DPDQ (3a) and DCDPDQ (3c) have a similar toxicity profile. Both compounds have an estimated LD50 of 136 mg/kg and are assigned to class III for acute oral toxicity (toxic if swallowed, $50 < LD50 \leq 300$). In comparison to the determined IC50 values for both compounds, the predicted toxicity class encompasses a wide concentration range, suggesting that both compounds are non-toxic. Importantly, the toxicity profile of both compounds was favorable, exhibiting no hepatotoxicity, nephrotoxicity, cardiotoxicity, or respiratory toxicity. Moreover, both compounds were inactive for induction of carcinogenicity, mutagenicity, cytotoxicity, immunotoxicity, clinical toxicity, and nutritional toxicity. However, both compounds were predicted to have active neurotoxicity with probabilities ranging from 0.7-0.77 and blood-brain barrier (BBB) permeability ranging from 0.93-0.97. Crucially, neither the toxicological signalling pathways listed in the Tox21 dataset nor toxicological targets from the Novartis in vitro safety panels used in the analysis showed activity for the induction of such less probable toxicity. Furthermore, drug metabolising enzymes like CYP1A2, CYP2C19, and CYP2C9 were shown to be active for metabolism of both compounds, but have probability less than 0.7 and therefore

DOI: https://doi.org/10.17509/ijost.v11i2.89682
p- ISSN 2528-1410 e- ISSN 2527-8045

considered less probable to cause toxicity. Overall, both compounds emerged as promising candidates with favorable toxicity profiles, characterized by lack of major organ toxicities and low predicted oral toxicity.

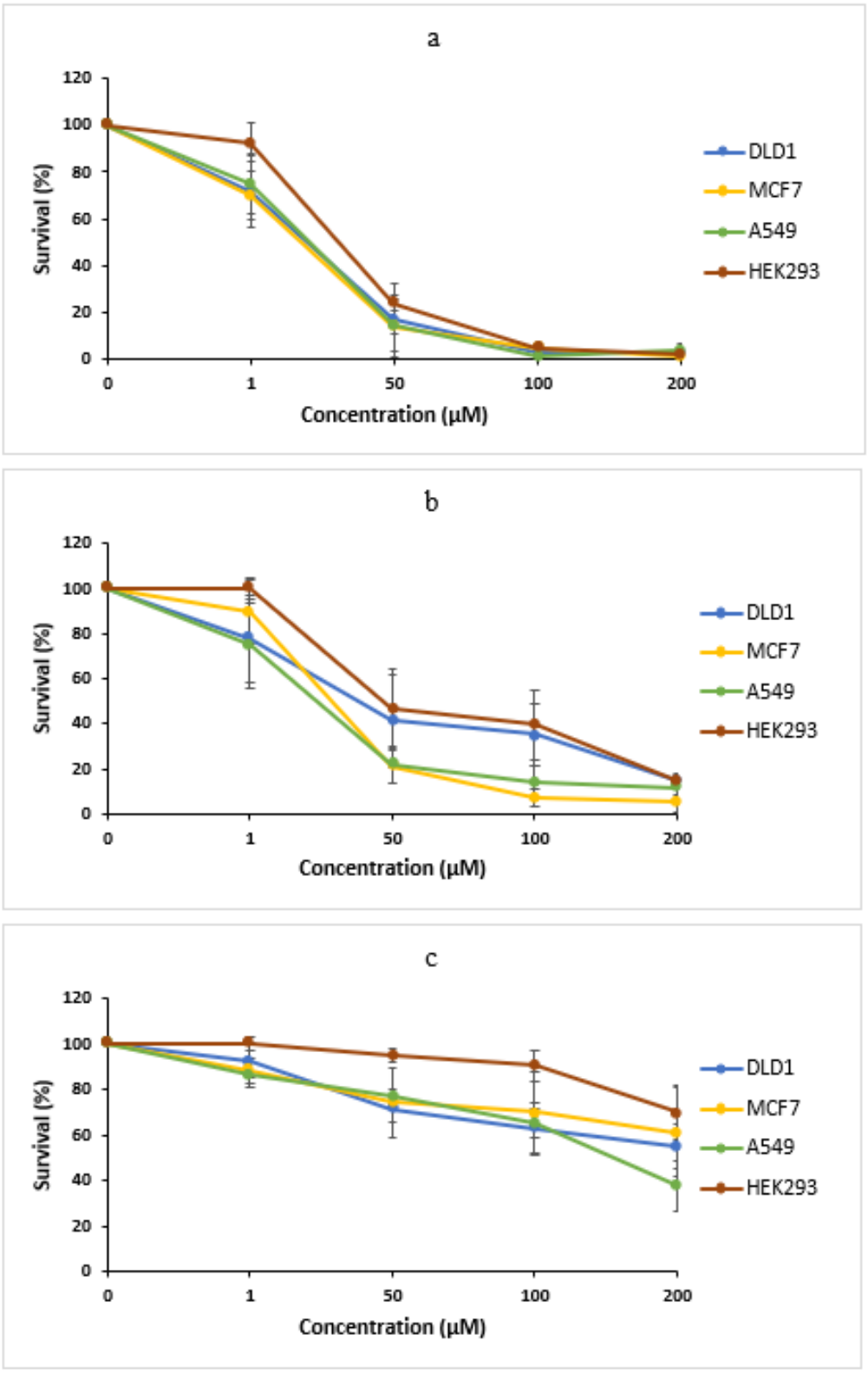

Figure 10. Concertation-dependent anti-cancer activity of (a) DPDQ (3a), (b) DCDPDQ (3c), and (c) DNDPDQ 3b displayed by cancer cell lines (MCF-7, DLD1, and A549) and non-cancerous cells (HEK293) for 96 h treatment.

DOI: https://doi.org/10.17509/ijost.v11i2.89682
p- ISSN 2528-1410 e- ISSN 2527-8045

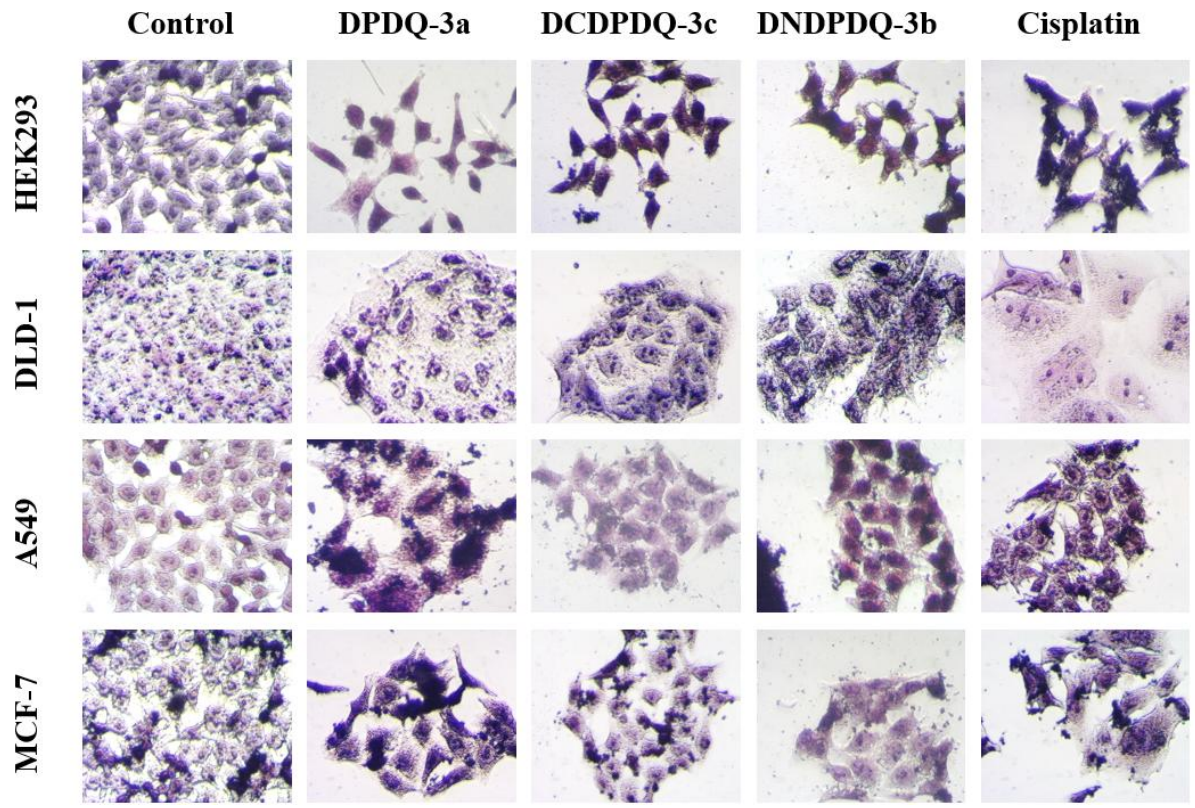

Figure 11. Anti-cancer activity of DPDQ derivatives and cisplatin against cancer cell lines (MCF-7, DLD1, and A549) and non-cancerous cells (HEK293) for 96h treatment. Each cell line was treated at the respective IC50 as indicated in Table 2. (40× objective lens).

3.5. Molecular Docking

The objective of this study was to accurately simulate the internal dynamics of infected cells following treatment with the proposed inhibitors. To accomplish this, the MOE module was employed to carry out molecular docking simulations between the inhibitors Diphenyldiquinoline (DPDQ)-3a and Dinitrovdiphenyldiquinoline (DNDPDQ)-3b and the PDB co-crystal structure 5KVT of anti-tumor agents [64]. **Table 3** presents a summary of the binding energy scores and details the interactions between the functional groups of the compounds and the protein residues [65].

Table 3. Results of molecular docking for two compounds with the target protein.

Compounds	PDB ID	Activity	Energy (kcal/mol)	Bonds formed between functional groups of the component and protein residues	
				Functional groups	Residues
Diphenyldiquinoline (DPDQ)-3a	5KVT	Anti-Tumor Agents	-7.6209	Benzene	Asp 599 and Val 524
Dinitrovdiphenyldiquinoline (DNDPDQ)-3b			-7.7664	Benzene	Val 524, Gly 595, and Gly 517

Figure 12 displays images of the docking complexes. **Table 3** presents details of the ligand types (hydrogen bonding interaction centers) and their corresponding protein receptors. The

DOI: https://doi.org/10.17509/ijost.v11i2.89682
p- ISSN 2528-1410 e- ISSN 2527-8045

table also includes the functional groups interacting with the enzymes, as well as the calculated binding energies for the molecular docking simulation.

The energy values (S) you've reported suggest that compounds 3A and 3B have a strong binding affinity for the targeted protein (5KVT). Generally, lower (more negative) energy values indicate more favorable interactions and higher binding affinities. If these scores are derived from docking studies or similar computational methods, they imply that both compounds have a potentially effective interaction with the protein, which could be promising for their activity against tumors.

Figure 12 shows that molecule 3A forms bonds with residues Asp 599 and Val 524, while molecule 3B interacts with residues Val 524, Gly 595, and Gly 517. These varied interactions illustrate the potential inhibitory effects of these compounds on the targeted protein 5KVT. The strong interactions observed between these synthesized molecules and the target protein suggest their potential as anti-cancer drugs. Such promising affinity toward the targeted protein is a key characteristic for developing effective anti-cancer agents.

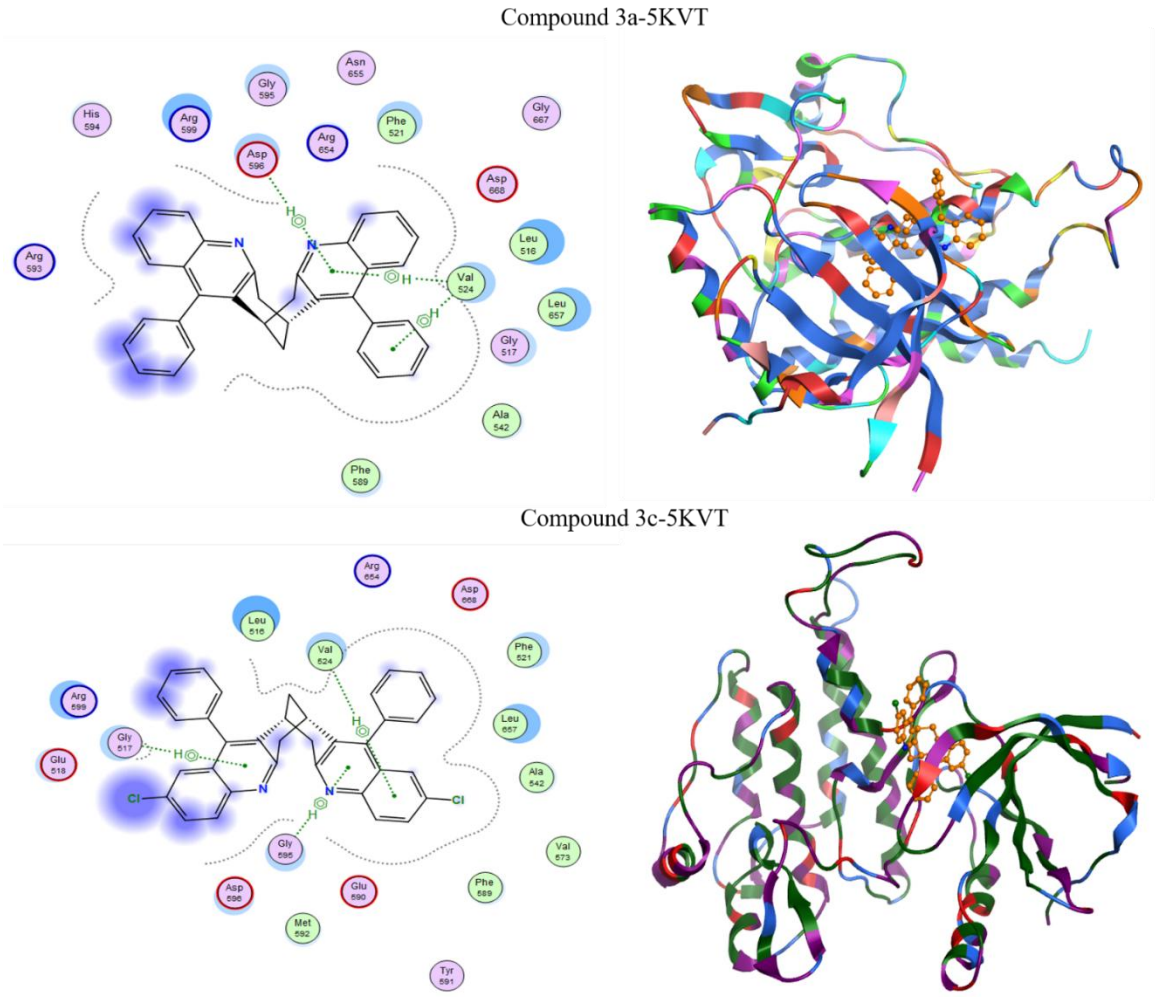

Figure 12. Best docking interaction of synthesized compounds and the target protein 5KVT.

4. CONCLUSION

This article showcases the therapeutic abilities of new diphenyldiquinoline derivatives (DPDQ-3a, DNDPDQ-3b, and DCDPDQ-3c) as selective and efficient anti-tumor agents. The prepared compounds revealed cytotoxicity in a concentration-dependent manner against several cancer cell lines, with DPDQ-3a being the most effective and selective. In comparison

DOI: https://doi.org/10.17509/ijost.v11i2.89682
p- ISSN 2528-1410 e- ISSN 2527-8045

with the reference drug cisplatin, DPDQ-3a exhibited the most potent antiproliferative effects against lung, colorectal, and breast cancer cells with the least cytotoxicity toward normal cells.

The results from molecular docking studies confirmed the strong binding of DPDQ-3a and DNDPDQ-3b with some tumor-specific protein targets, thereby pointing out their potential as inhibitors of cancer-related pathways. In silico toxicology predictions further foretold safety profiles for both DPDQ-3a and DCDPDQ-3c, with no major organ toxicity or cancerogenicity, even though the former showed it to be safe, while the latter was malignant.

The intermolecular interactions in the crystal structures were also investigated through Hirshfeld surface analysis, which provided further insight into the molecular interactions and stability of the compounds. The attachment of functional groups, for instance, nitro and chloro substituents, has played a crucial role in the alteration of the biological activity and the high selectivity of these derivatives, which underscores the crucial role that structural modifications play in their pharmacological properties. Moreover, the extraordinary results of this research underscore the compilation of experimental and computational approaches for the development of more effective cancer Nano-therapy.

All in all, this research lays the groundwork for the future preclinical examination of quinoline-derived compounds as antitumor agents. Subsequent investigations may look into these derivatives to make sure they are as strong and as fast in their action as they can be, and study them using combination chemotherapy.

5. ACKNOWLEDGMENTS

The authors gratefully acknowledge the Deanship of Scientific Research – Mutah University, Jordan, for supporting this work. This study was funded by a research grant from Mutah University (Decision no. 766/2023). The funders had no role in study design, data collection and analysis, decision to publish, or preparation of the manuscript.

6. AUTHORS' NOTE

The authors declare that there is no conflict of interest regarding the publication of this article. The authors confirmed that the paper was free of plagiarism.

7. REFERENCES

[1] Wahyuni, W., Diantini, A., Ghozali, M., Subarnas, A., Julaeha, E., Amalia, R., Fristiohady, A., Sundowo, A., Fajriah, S., Hadisaputri, Y.E., Febrianti, R.M., Azzahra, F., and Sahidin, I. (2022). In-vitro anticancer activity of chemical constituents from etlingera alba poulsen against triple negative breast cancer and in silico approaches towards matrix metalloproteinase-1 inhibition. *Indonesian Journal of Science and Technology*, *7*(2), 251-278.

[2] Fauziah, R.R., Rie, C., Yoshino, T., Ogita, S., and Yamamoto, Y. (2022). Anti-Cancer effect of phosphatidylcholine containing conjugated linoleic acid at sn-2 position on MCF-7 breast cancer cell line. *Indonesian Journal of Science and Technology*, *7*(2), 279-290.

[3] Fristiohady, A., Asasutjarit, R., Purnama, L.O.M.J., Theeramunkong, S., Al-Ramadan, W., Haruna, L.A., Rahmatika, N.S., Baharum, S.N., and Sahidin, I. (2022). Phytochemical profile and anticancer activity from medicinal plants against melanoma skin cancer: A Review. *Indonesian Journal of Science and Technology*, *7*(3), 405-470.

DOI: https://doi.org/10.17509/ijost.v11i2.89682
p- ISSN 2528-1410 e- ISSN 2527-8045

[4] Yousaf, A., Tasneem, N., Mustafa, A., Fatima, R., Nabia, N., Khan, R.A., Abdulbasit, H., Abubakar, M., Asadullah, A., Rizwan, R., and Baqa-ur-Rehman, B. (2021). Gastric cancer associated risk factors and prevalence in Pakistan. *ASEAN Journal of Science and Engineering*, *1*(2), 73-78.

[5] Obiwusi, K.Y., Olatunde, Y.O., Afolabi, G.K., Oke, A., Oyelakin, A.M., and Salami, A. (2023). Evaluating the performance of supervised machine learning algorithms in breast cancer datasets. *ASEAN Journal of Science and Engineering*, *3*(2), 179-184.

[6] Tfayli, A.H., El-Halabi, L.N., and Khuri, F.R. (2025). Global disparities in cancer care: bridging the gap in affordability and access to medications between high and low-income countries. *Cancer*, *131*, e35590.

[7] Thanneeru, V.S. and Panigrahi, N. (2025). Novel quinoline nitrate derivatives: synthesis, characterization, and evaluation of their anticancer activity with a focus on molecular docking and no release. *Anti-Cancer Agents in Medicinal Chemistry*, *25*, 272–280.

[8] Kumaraswamy, B., Hemalatha, K., Pal, R.; Matada, G.S.P., Hosamani, K.R., Aayishamma, I., and Aishwarya, N.V.S.S. (2024). An insight into sustainable and green chemistry approaches for the synthesis of quinoline derivatives as anticancer agents. *European Journal of Medicinal Chemistry*, *275*, 116561.

[9] Wu, Y.-C., Lu, M.-T., Kuo, S.-C., Chu, P.-C., and Chang, C.-S. (2024). Synthesis and SAR investigation of biphenylaminoquinoline derivatives with benzyloxy substituents as promising anticancer agents. *Chemical Biology & Drug Design*, *103*, e14509.

[10] Lakhrissi Y., Rbaa M., Tuzun B., Hichar A., Anouar E.H., Ounine K., Almalki F., Ben Hadda T., and Zarrouk A., Lakhrissi B. (2022), Synthesis, structural confirmation, antibacterial properties and bio-informatics computational analyses of new pyrrole based on 8-hydroxyquinoline. *Journal of Molecular Structure*, *1259*, 132683.

[11] Tyagi, S., Salahuddin, Mazumder, A., Kumar, R., Datt, V., Shabana, K., and Ahsan, M. J. (2023). Synthesis and SAR of Potential Anti-Cancer Agents of Quinoline Analogues: A Review. *Medicinal Chemistry*, *19*(8), 785-812.

[12] Diass, K., Oualdi, I., Dalli, M., Azizi, S.E., Mohamed, M., Gseyra, N., Touzani, R., and Hammouti, B. (2023). Artemisia herba alba essential oil: GC/MS analysis, antioxidant activities with molecular docking on S protein of SARS-CoV-2. *Indonesian Journal of Science and Technology*, *8*(1), 1-18.

[13] El Mrayej, H., En-Nabety, G., Ettahiri, W., Jghaoui, M., Sabbahi, R., Hammouti, B., Rais, Z. and Taleb, M. (2025). Triazolopyrimidine derivatives: A comprehensive review of their synthesis, reactivity, biological properties, and molecular docking studies. *Indonesian Journal of Science and Technology*, *10*(1), 41-74.

[14] Hendrarti, W., Umar, A.H., Syahruni, R., Rafi, M., and Kusuma, W.A. (2024). Deciphering the mechanism of action cosmos caudatus compounds against breast neoplasm: A combination of pharmacological networking and molecular docking approach with bibliometric analysis. *Indonesian Journal of Science and Technology*, *9*(2), 527-556.

[15] Abbas, S. K., Jaafar, M. T., Ali, H. R., and Alsarayreh, A. A. (2024). Synthesis, antibacterial evaluation and molecular docking of 2,4,5-tri-imidazole derivatives. *Moroccan Journal of Chemistry, 13*(2), 1222–1239.

[16] Abdessadak, O., Hajji, H., Mehanend, S., Lakhlifi, T., and Bouachrine, M. (2022). Reverse docking on five original PPO structures: Plant, bacterial, and human. *Moroccan Journal of Chemistry*, *10*(3), 442–451.

[17] Abu-Rayyan, A., Shalalin, K., Suleiman, M., Warad, I., and Sawatfa, A. (2024). Synthesis, optimization, DFT/TD-DFT and COX/LOX docking of new Schiff base N'-((9-ethyl-9H-

DOI: https://doi.org/10.17509/ijost.v11i2.89682
p- ISSN 2528-1410 e- ISSN 2527-8045

carbazol-1-yl)methylene)naphthalene-2-sulfonohydrazide. *Moroccan Journal of Chemistry*, *12*(1), 78–88.

[18] Abu-Rayyan, A., Suleiman, M., Daraghmeh, A., Sawatfa, A., and Warad, I. (2023). Synthesis, characterization, E/Z-isomerization, DFT, optical and IBNA docking of new Schiff base derived from naphthalene-2-sulfonohydrazide. *Moroccan Journal of Chemistry*, *11*(3), 613–622.

[19] Ahamed, L. S., Sallal, Z. A., Al-Jelaiwi, O. H. R., Shamaya, A. N. S., and Mahmood, A. A. R. (2025). Design, synthesis, and biological evaluation of new sulfonamides derived from 2-aminopyridine: Molecular docking, POM analysis, and identification of the pharmacophore sites. *Moroccan Journal of Chemistry*, *13*(2), 519–539.

[20] Ainane, A., Abdoul-Latif, F. M., Achenani, L., Ben Hadda, T., & Ainane, T. (2025). Computational approaches to Spirulina platensis growth with urea-derived nanonutrients: Thermodynamic properties, energetic profiles, molecular docking and POM analysis of pharmacophore sites. *Moroccan Journal of Chemistry*, *13*(3), 1210–1227.

[21] Ali, F. J., Radhi, E. R., Kadhium, A. J., and Ali, K. J. (2023). Preparation and characterization of new mixed azo ligand complexes with some metal ions and in vitro biological activity and molecular docking study of their Ni(II) and Hg(II) complexes. *Moroccan Journal of Chemistry*, *11*(4), 965–978.

[22] Aoumer, N., Tchouar, N., Belaidi, S., Lanez, T., and Chitta, S. (2021). Molecular docking studies for the identifications of novel antimicrobial compounds targeting Staphylococcus aureus. *Moroccan Journal of Chemistry*, *9*(2), 274–289.

[23] Bekkouch, A., Mostafi, H. E., Merzouki, M., Challouqi, A., & Mesfioui, A. (2024). Potential inhibition of ALDH by argan oil compounds, computational approach by docking, ADMET and molecular dynamics. *Moroccan Journal of Chemistry*, *12*(2), 676–695.

[24] Bouamrane, S., Khaldan, A., Hajji, H., Bouachrine, M., & Lakhlifi, T. (2022). 3D-QSAR, molecular docking, molecular dynamic simulation, and ADMET study of bioactive compounds against Candida albicans. *Moroccan Journal of Chemistry*, *10*(3), 523–541.

[25] Boumezzourh, A., Ouknin, M., Merzouki, M., Umoren, S. A., & Majidi, L. (2023). Acetylcholinesterase, tyrosinase, α-glucosidase inhibition of Ammoides leucotrichus Coss. & Dur. fruits essential oil and ethanolic extract and molecular docking analysis. *Moroccan Journal of Chemistry*, *11*(4), 1287–1298.

[26] Daoui, O., El Mouhi, R., Barghady, F., Elkhaldi, R., and Benjelloun, A. T. (2022). 3D-QSAR modeling, molecular docking and drug-like properties investigations of novel heterocyclic compounds derived from Magnolia officinalis as hit compounds against NSCLC. *Moroccan Journal of Chemistry*, *10*(4), 881–890.

[27] Filali, M., Lahyaoui, M., Bahsis, L., Kandri Rodi, Y., and El-Hadrami, E. M. (2024). Novel triazole-pyrazine as potential antibacterial agents: Synthesis, characterization, antibacterial activity, drug-likeness properties and molecular docking studies. *Moroccan Journal of Chemistry*, *13*(2), 1367–1379.

[28] Haddou, S., Mounime, K., Loukili, E. H., Hammouti, B., and Chahine, A. (2023). Investigating the biological activities of Moroccan Cannabis sativa L. seed extract: Antimicrobial, anti-inflammatory, and antioxidant effects with molecular docking analysis. *Moroccan Journal of Chemistry*, *11*(4), 1116–1136.

[29] İslamoğlu, E., and Hacfazlıoğlu, E. (2022). Investigation of the usability of some triazole derivative compounds as drug active ingredients by ADME and molecular docking properties. *Moroccan Journal of Chemistry*, *10*(4), 861–880.

DOI: https://doi.org/10.17509/ijost.v11i2.89682
p- ISSN 2528-1410 e- ISSN 2527-8045

[30] Khaldan, A., Bouamrane, S., El-Mernissi, R., Bouachrine, M., and Lakhlifi, T. (2022). In silico design of new α-glucosidase inhibitors through 3D-QSAR study, molecular docking modeling and ADMET analysis. *Moroccan Journal of Chemistry*, *10*(1), 22–36.

[31] Khaldan, A., Bouamrane, S., El-Mernissi, R., Lakhlifi, T., and Sbai, A. (2022). In search of new potent α-glucosidase inhibitors: Molecular docking and ADMET prediction. *Moroccan Journal of Chemistry*, *10*(4), 772–786.

[32] Koubi, Y., Hajji, H., Moukhliss, Y., Bouachrine, M., and Lakhlifi, T. (2022). In silico studies of 1,4-disubstituted 1,2,3-triazole with amide functionality: Antimicrobial evaluation against Escherichia coli using 3D-QSAR, molecular docking, and ADMET properties. *Moroccan Journal of Chemistry*, *10*(4), 689–702.

[33] Merzouki, M., Bourassi, L., Abidi, R., Sabbahi, R., and Challouqi, A. (2024). Deciphering the SARS-CoV-2 Delta variant: Antiviral compound efficacy by molecular docking, ADMET, and dynamics studies. *Moroccan Journal of Chemistry*, *12*(3), 1153–1171.

[34] Ravichandran, V., Raghuraman, S., Prabha, T., Harish, R., and Parasuraman, P. (2025). In silico docking, drug-likeness and toxicity prediction studies of bioactive compounds of Eurycoma longifolia as potential multi-targeted antiviral agents against SARS-CoV-2. *Moroccan Journal of Chemistry*, *13*(1), 381–404.

[35] Riouchi, O., Bouroumane, N., Boutaybi, M. E., Bouyanzer, A., and Touzani, R. (2025). Extract and molecular docking: Exploring the oxidation of 3,5-di-tert-butylcatechol and 2-aminophenol in the presence of O_2 from air: Towards valuable organic compounds. *Moroccan Journal of Chemistry*, *13*(1), 145–167.

[36] Sabour, A., Elsabhani, A., Maymoun, G., Kazzaoui, S. E., and El-Maimouni, L. (2024). Synthesis, structural and crystallographic characterization of new hydrosoluble thymol derivatives with enhanced antioxidant activity assessed by docking study. *Moroccan Journal of Chemistry*, *12*(3), 554–569.

[37] Safi, M. N., Ahamed, L. S., Almalki, F. A., and Hadda, T. B. (2025). Synthesis, anticancer, antimicrobial evaluation, in silico molecular docking and POM analyses of new 4,7-dimethyl coumarin containing sulfonamides. *Moroccan Journal of Chemistry*, *13*(2), 849–880.

[38] Seggat, Y., Hafez, B., Lahyaoui, M., Chahdi, F. O., and Sebbar, N. K. (2024). Synthesis, spectroscopic characterization, cytotoxic activity, ADME prediction and molecular docking studies of the novel series quinoxaline-2,3-dione. *Moroccan Journal of Chemistry*, *13*(3), 1323–1349.

[39] Shrestha, R. L. S., Panta, R., Maharjan, B., Marasini, B. P., and Subin, J. A. (2024). Molecular docking and ADMET prediction of compounds from Piper longum L. detected by GC-MS analysis in diabetes management. *Moroccan Journal of Chemistry*, *12*(2), 776–798.

[40] Tabti, K., El Mchichi, L., Moukhliss, Y., Bouachrine, M., and Lakhlifi, T. (2022). CoMFA topomer, CoMFA, CoMSIA, HQSAR, docking molecular, dynamique study and ADMET study on phenoxypropyl isoxazole derivatives for coxsackie virus B3 virus inhibitors activity. *Moroccan Journal of Chemistry*, *10*(4), 703–725.

[41] Yaqoubi, M. E., Hafez, B., Lahyaoui, M., Rodi, Y. K., and Sebbar, N. K. (2025). Computational insights into benzothiophene derivatives as potential antibiotics against multidrug-resistant Staphylococcus aureus: QSAR modeling and molecular docking studies. *Moroccan Journal of Chemistry*, *12*(2), 774–806.

[42] Alshahateet, S.F., Bhadbhade, M.M., Bishop, R., and Scudder, M.L. (2014). Different solvents yield alternative crystal forms through aromatic, halogen bonding and hydrogen bonding competition. *CrystEngComm*, *17*, 877–888.

DOI: https://doi.org/10.17509/ijost.v11i2.89682
p- ISSN 2528-1410 e- ISSN 2527-8045

[43] Alshahateet, S.F., Ong, T.T., Bishop, R., Kooli, F., and Messali, M. A. (2006). Dinitrodiphenyldiquinoline host for selective inclusion of polar guests. *Crystal Growth & Design*, *6*, 1676–1683.
[44] Spackman, P. R., Turner, M. J., McKinnon, J. J., Wolff, S. K., Grimwood, D. J., Jayatilaka, D., and Spackman, M. A. (2021). CrystalExplorer: a program for Hirshfeld surface analysis, visualization and quantitative analysis of molecular crystals. *Applied Crystallography*, *54*(3), 1006-1011.
[45] Spackman, M. A., and McKinnon, J. J. (2002). Fingerprinting intermolecular interactions in molecular crystals. *CrystEngComm*, *4*(66), 378-392.
[46] Spackman, M. A., and Jayatilaka, D. (2009). Hirshfeld surface analysis. *CrystEngComm*, *11*(1), 19-32.
[47] Fiandini, M., Nandiyanto, A.B.D., Al Husaeni, D.F., Al Husaeni, D.N., and Mushiban, M. (2024). How to calculate statistics for significant difference test using SPSS: Understanding students comprehension on the concept of steam engines as power plant. *Indonesian Journal of Science and Technology*, *9*(1), 45-108.
[48] Rahayu, N.I., Muktiarni, M., and Hidayat, Y. (2024). An application of statistical testing: A guide to basic parametric statistics in educational research using SPSS. *ASEAN Journal of Science and Engineering*, *4*(3), 569-582.
[49] Afifah, S., Mudzakir, A., and Nandiyanto, A.B.D. (2022). How to calculate paired sample t-test using SPSS software: From step-by-step processing for users to the practical examples in the analysis of the effect of application anti-fire bamboo teaching materials on student learning outcomes. *Indonesian Journal of Teaching in Science*, *2*(1), 81-92.
[50] Banerjee, P., Kemmler, E., Dunkel, M., and Preissner, R. (2024). ProTox 3.0: a webserver for the prediction of toxicity of chemicals. *Nucleic Acids Research*, *52*(W1), W513-W520.
[51] Banerjee, P., Eckert, A. O., Schrey, A. K., and Preissner, R. (2018). ProTox-II: a webserver for the prediction of toxicity of chemicals. *Nucleic Acids Research*, *46*(W1), W257-W263.
[52] Vilar, S., Cozza, G., and Moro, S. (2008). Medicinal chemistry and the molecular operating environment (MOE): Application of QSAR and molecular docking to drug discovery. *Current Topics in Medicinal Chemistry*, *8*(18), 1555-1572.
[53] Noguchi, T., Akiyama, Y. (2003). PDB-REPRDB: A database of representative protein chains from the protein data bank (PDB) in 2003. *Nucleic Acids Research*, *31*, 492–493.
[54] Er-rajy, M., Fadili, M.E., Mujwar, S., Lenda, F.Z., Zarougui, S., and Elhallaoui, M. (2023). QSAR, molecular docking, and molecular dynamics simulation–based design of novel anti-cancer drugs targeting thioredoxin reductase enzyme. *Structural Chemistry*, *34*, 1527–1543.
[55] Er-Rajy, M., El Fadili, M., Mujwar, S., Zarougui, S., & Elhallaoui, M. (2023). Design of novel anti-cancer drugs targeting TRKs inhibitors based 3D QSAR, molecular docking and molecular dynamics simulation. *Journal of Biomolecular Structure and Dynamics*, *41*(21), 11657-11670.
[56] Haddou, S., Mounime, K., Loukili, E., Ou-Yahia, D., Hbika, A., Idrissi, M. Y., and Chahine, A. (2023). Investigating the biological activities of Moroccan Cannabis sativa L seed extracts: Antimicrobial, anti-inflammatory, and antioxidant effects with molecular docking analysis. *Moroccan Journal of Chemistry*, *11*(04), 1116-1136.
[57] Althagafi, I., El-Metwaly, N., and Farghaly, T.A. (2019). New series of thiazole derivatives: Synthesis, structural elucidation, antimicrobial activity, molecular modeling and MOE docking. *Molecules*, 24, 1741.

DOI: https://doi.org/10.17509/ijost.v11i2.89682
p- ISSN 2528-1410 e- ISSN 2527-8045

[58] Yuan, C., Wang, M.-H., Wang, F., Chen, P.-Y., Ke, X.-G., Yu, B., Yang, Y.-F., You, P.-T., and Wu, H.-Z. (2021). Network pharmacology and molecular docking reveal the mechanism of scopoletin against non-small cell lung cancer. *Life Sciences 2021*, *270*, 119105,

[59] Hidaoui, S., Hamdi, N., Akouibaa, M., Benali-Cherif, R., Vaclav, E., Dusek, M., Lachkar, M., and El Bali, B. (2022). Synthesis, Crystal Structure and Catalytic Activity of the New Hybrid Phosphate (C4H12N2)[Co(H2O)6](HPO4)2. *Journal of Molecular Structure*, *1265*, 133296.

[60] Hidaoui, S., Hamdi, N., Saadi, M., El Omari, M., Pui, A., El Bali, B., El Ammari, L., and Lachkar, M. (2025). Structural study, spectroscopic characterization, thermal decomposition, hirshfeld surface analysis, and antibacterial activity of a novel hybrid centrosymmetric material (C4H12N2)[Co(H2O)2(H2P2O7)2].2H2O. *Inorganic Chemistry Communications*, *174*, 114002.

[61] Zerrouk, M., Ariba, Z., Hidaoui, S., Bouayad, A., Ouarsal, R., Poupon, M., and El Bali, B. (2025). Hybrid-phosphite (C2H10N2)[Zn3 (H2PO3) 4 (HPO3) 2.2 H2O]: Crystal structure, catalytic activity, and Hirshfeld surface analysis. *Journal of Molecular Structure*, *1327*, 141233.

[62] Abuelizz, H.A., Taie, H.A.A., Bakheit, A.H., Marzouk, M., Abdellatif, M.M., and Al-Salahi, R. (2021). Biological evaluation of 4-(1H-Triazol-1-Yl)benzoic acid hybrids as antioxidant agents: In vitro screening and dft study. *Applied Sciences*, *11*, 11642.

[63] Al-Taweel, S., Al-Saraireh, Y., Al-Trawneh, S., Alshahateet, S., Al-Tarawneh, R., Ayed, N.; Alkhojah, M., AL-Khaboori, W.; Zereini, W., and Al-Qaralleh, O. (2023). Synthesis and biological evaluation of ciprofloxacin – 1,2,3-triazole hybrids as antitumor, antibacterial, and antioxidant agents. *Heliyon*, *9*, e22592.

[64] Youssef, A.M.M.; Maaty, D.A.M.; and Al-Saraireh, Y.M. (2023). Phytochemical analysis and profiling of antioxidants and anticancer compounds from tephrosia purpurea (L.) subsp. apollinea family fabaceae. *Molecules*, *28*, 3939.

[65] Drilon, A., Siena, S., Ou, S. H. I., Patel, M., Ahn, M. J., Lee, J., and De Braud, F. G. (2017). Safety and antitumor activity of the multitargeted pan-TRK, ROS1, and ALK inhibitor entrectinib: combined results from two phase I trials (ALKA-372-001 and STARTRK-1). *Cancer Discovery*, *7*(4), 400-409.

DOI: https://doi.org/10.17509/ijost.v11i2.89682
p- ISSN 2528-1410 e- ISSN 2527-8045